Electrical transport, thermal transport, and elastic properties of M_2AlC (M=Ti, Cr, Nb, and V)

J. D. Hettinger,[1] S. E. Lofland,[1] P. Finkel,[1,*] T. Meehan,[1] J. Palma,[1] K. Harrell,[1] S. Gupta,[2] A. Ganguly,[2] T. El-Raghy,[3] and M. W. Barsoum[2]

[1]*Department of Physics and Astronomy, Rowan University, Glassboro, New Jersey 08028, USA*

[2]*Department of Materials Engineering, Drexel University, Philadelphia, Pennsylvania 19104, USA*

[3]*3ONE2, Voorhees, New Jersey 08043, USA*

(Received 1 April 2005; published 27 September 2005)

In this paper we report on a systematic investigation, in the 5 to 300 K temperature regime, of the electronic, magnetotransport, thermoelectric, thermal, and elastic properties of four M_2AlC phases: Ti_2AlC, V_2AlC, Cr_2AlC, and Nb_2AlC. The electrical conductivity, Hall coefficient, and magnetoresistances are analyzed within a two-band framework assuming a temperature-independent charge carrier concentration. As with other *MAX*-phase materials, these ternaries are nearly compensated, viz. the densities and mobilities of electrons and holes are almost equal. There is little correlation between the Seebeck and Hall coefficients. With Young's and shear moduli in the 270 GPa and 120 GPa range, respectively, the phases studied herein are reasonably stiff. With room temperature thermal conductivities in the 25 W/m K range (45 W/m K for V_2AlC) they are also good thermal conductors.

DOI: 10.1103/PhysRevB.72.115120 PACS number(s): 72.15.Eb, 72.15.Gd, 72.15.Jf, 62.20.Dc

I. INTRODUCTION

Recent interest in an unusual class of 50+ layered ternary carbides and nitrides has been generated as a result of the densification and characterization of phase-pure samples with the general chemical formula: $M_{n+1}AX_n$ where $n=1$ to 3, M is an early transition metal, A is an A-group element (mostly IIIA and IVA), and X is either C and or N.[1] Most of these ternaries were first synthesized in powder form more than 35 years ago,[2] yet little was known about their properties until recently. Partially because these materials are comprised of $M_{n+1}X_n$ layers interleaved with pure A layers, and partially because of how they deform they are best described as nanolaminates. As a result of this layered structure they are readily machinable, despite the fact that some of them are elastically quite stiff, as well as lightweight.[3] They are also excellent electric and thermal conductors.[1] When combined with the low friction coefficients associated with their basal planes,[4] and the excellent oxidation resistances of some of them,[5,6] their potential in applications such as rotating contacts at elevated temperatures becomes obvious.

To date, by far the most studied of this group of materials is Ti_3SiC_2.[7,8] Some work has been geared toward understanding the properties of Ti_3AlC_2 and Ti_4AlN_3 (Ref. 9) and, to a lesser extent, Ti_3GeC_2.[10,11] Yet much of the interesting physics leading to the properties of these materials can best be evaluated and understood through systematic investigations of the materials where the elemental constituents can be varied, while maintaining the same crystallographic structure. One way to undergo such a systematic study is to investigate several different phases from the M_2AX group of *MAX*-phase materials. Over 40 M_2AX phases are known to exist: they include 11 different A-group elements and 9 different early transition metals. In fact, the structures more extensively studied, M_4AX_3 and M_3AX_2, are much more of an exception, consisting of only four known compounds. Recently we reported also on some elastic and electronic properties of some select *MAX* phases.[12]

In this paper—which is a continuation of our efforts in understanding the chemistry and/or physical property relationships in these compounds—we report on the 5 to 300 K electrical resistivities, Hall and Seebeck voltages, magnetoresistances, and thermal and elastic properties of the Al-containing phases: Ti_2AlC, V_2AlC, Cr_2AlC, and Nb_2AlC. Investigating this series allowed us to look for systematic trends when adding electrons across three columns of the periodic table (viz., Ti, V, Cr), while also attempting a comparison between elements in a single column (V and Nb).

II. EXPERIMENTAL DETAILS

Polycrystalline bulk samples of these phases were fabricated by reactively hot isostatically pressing a stoichiometric mixture of powders of the constituent elements. Details of the V_2AlC and Nb_2AlC syntheses are given elsewhere.[13,14] The Ti_2AlC and Cr_2AlC samples were made by pressureless sintering of prereacted powders. X-ray diffractometry indicated that the materials were predominantly phase pure. All samples were greater than 99% of their theoretical density.

Polycrystalline parallelepiped-shaped specimens with approximate dimensions $1\times1\times10$ mm^3 were cut from the bulk samples. The electrical resistivity ρ, Hall voltage V_H, and magnetoresistance $MR=[\rho(B)-\rho(0)]/\rho(0)$ were measured for temperatures T ranging between 5 and 300 K and magnetic fields B, up to 9 T with Quantum Design's Physical Properties Measurement System (PPMS). A specially designed sample holder—with spring-loaded gold-coated contacts—was used to mount the samples for electrical transport measurements. The voltage sensitivity was roughly 5 nV, and no contact heating was observed for currents up to 300 mA. Measurements were performed by a four-probe method to eliminate contact resistance for these low-resistivity materials. This configuration allowed a simultaneous measurement of the transverse and longitudinal magnetic-field-dependent voltages. The magnetoresistive

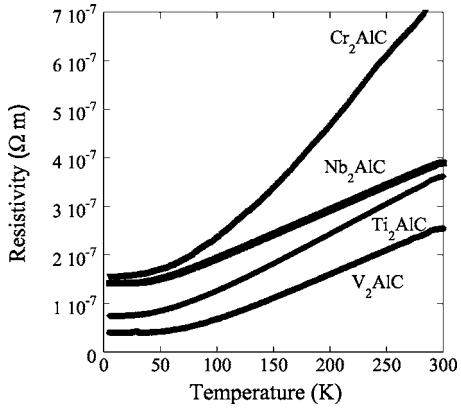

FIG. 1. Temperature dependence of resistivity.

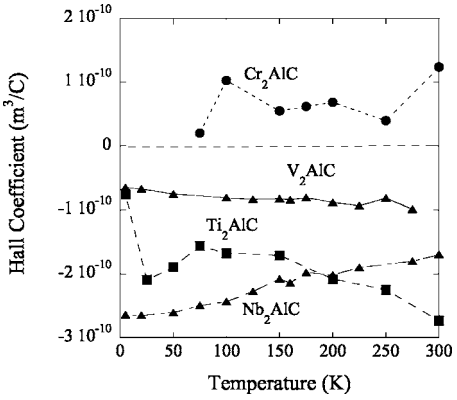

FIG. 2. Temperature dependence of Hall coefficients.

component of the measured voltage and extraction of the Hall signal were achieved by magnetic field reversal and subtraction of the measured voltages to separate those components even and odd in the magnetic field. Thermal voltages were eliminated from the measured values by use of a low-frequency ac current technique.

The Seebeck voltages were also measured using the PPMS configured with the thermal transport option (TTO) from 5 to 300 K in zero magnetic field. The TTO allows sequential measurements of the thermal conductivity, Seebeck voltage, and electrical resistivity at each temperature. This measurement was made by attaching four leads to the sample with conducting silver epoxy. A temperature gradient was established by applying heat at one end of the specimen while holding the other end at a constant temperature by maintaining good thermal contact with a low-temperature reservoir. Calibrated Cernox thermometers are attached to the sample between 4 and 7 mm apart. The temperature difference is monitored and the voltage measured at the same positions along the sample.

Ultrasonic measurements of elastic moduli were carried out using a RAM 10000 (RITEC) utilizing an echo-pulsed phase-sensitive detection technique for determining the time of flight (TOF) of the ultrasonic wave. This system was able to provide absolute and relative sound velocity measurements with a precision of 5 ppm. TOF of 10-MHz and 15-MHz tone bursts produced by a lithium niobate transducer were measured on $8\times8\times8$ mm^3 cubes cut from M_2AlC samples. In all cases phenyl salicylate was used as the ultrasonic transducer-bonding compound. Ultrasonic velocities were then used to calculate the bulk modulus, B, and Poisson's ratio, ν, assuming that the medium is isotropic.

III. RESULTS

Figure 1 presents the measured resistivities as a function of temperature. The slopes of the curves for the V-containing and Nb-containing materials are similar, with Nb_2AlC having a slightly higher overall resistivity. The Cr-containing and the Ti-containing materials have somewhat stronger temperature dependences. Of the materials measured, V_2AlC has the largest residual resistance ratio (RRR) [RRR $=\rho(300\ \mathrm{K})/\rho(5\ \mathrm{K})$] of about 6.5.

The Hall number, R_H, is plotted in Fig. 2 as a function of temperature. With the exception of Cr_2AlC for which R_H is slightly positive, R_H is negative. Although results for only one sample are shown for clarity, three samples of Cr_2AlC were measured all showing a small positive Hall number. Also observed in Fig. 2 are the temperature dependences of R_H. Note that some tend toward zero as the temperature is lowered, while Nb_2AlC becomes more negative as the temperature is decreased.

Figure 3(a) is a plot of α which is related to the relative change in resistivity with applied magnetic field, B [see Eq. (2) below]. The temperature dependencies of the Seebeck voltages are shown in Fig. 4. In general they are low and tend to fluctuate around zero and change sign with increasing temperatures.

The thermal conductivity results are shown in Fig. 5(a). The conductivities rise rapidly in the 5–100 K temperature range and then tend to plateau. At $\approx$22 W/m K, the room temperature conductivity κ of Cr_2AlC is the lowest measured; at $\approx$48 W/m K, that of V_2AlC is the highest, with those of Ti_2AlC and Nb_2AlC in between. Figure 5(b) plots the temperature dependence of the Lorenz number $L=\rho\kappa/T$. Note that at higher temperatures, the Lorenz number for Nb_2AlC asymptotically approaches the horizontal line drawn at $L_0=2.45\times10^{-8}$ V^2/K^2, which represents the value of the Lorenz number when the phonon contribution to the total thermal conductivity is negligible.

IV. DISCUSSION

A. Electronic properties

The resistivities for all materials investigated herein drop linearly with decreasing temperatures (Fig. 1). This metallike behavior, characteristic of all *MAX* phases explored to date,[15,10] results from the large density of states at the Fermi level $N(E_F)$ of these solids.[12,16]

To shed further light on the mechanisms of electronic conduction in these solids, it is useful to analyze the magnetotransport and electrotransport results. A temperature-dependent Hall number requires at least a two-band model to explain the results. Within a two-band framework, the expression used to describe the Hall number R_H is

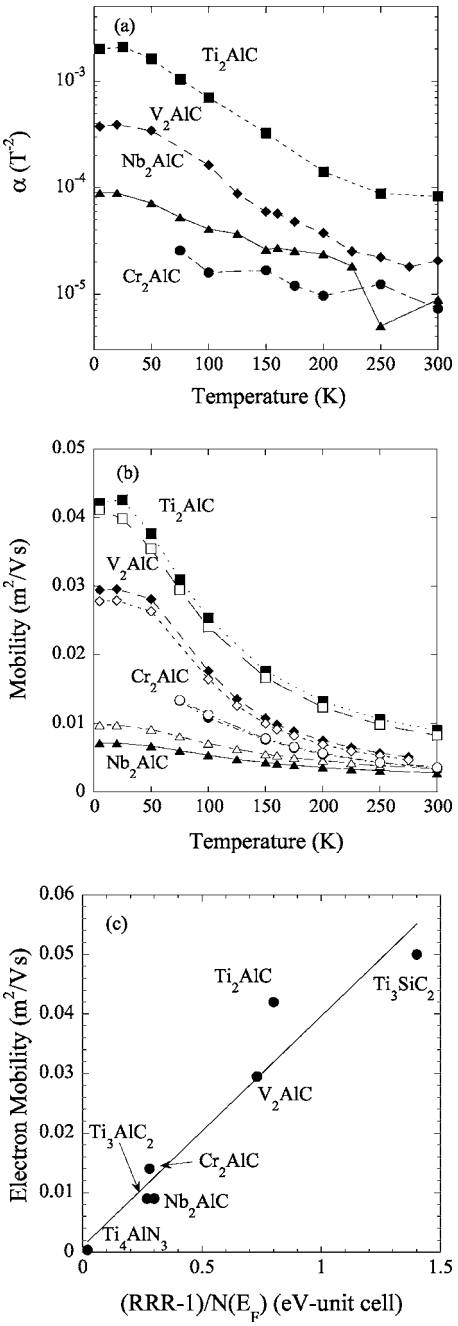

FIG. 3. (a) Semilogarithmic plot of α as a function of temperature for several M_2AlC materials. The parameter α was extracted assuming $\Delta\rho/\rho(B=0)=\alpha B^2$. (b) Temperature dependence of electron (solid symbols) and hole (open symbols) mobilities. (c) Mobilities at 4 K versus $(\mathrm{RRR}-1)/N(E_F)$. The linear relationship indicates the electron-phonon coupling is similar in all studied *MAX* phases.

$$R_H = \frac{(\mu_p^2 p - \mu_n^2 n)}{e(\mu_p p + \mu_n n)^2}. \tag{1}$$

This expression contains four unknowns: μ_p, μ_n, p, and n which are the hole and electron mobilities and the hole and electron concentrations, respectively. To solve completely for each unknown, three additional constraints are required.

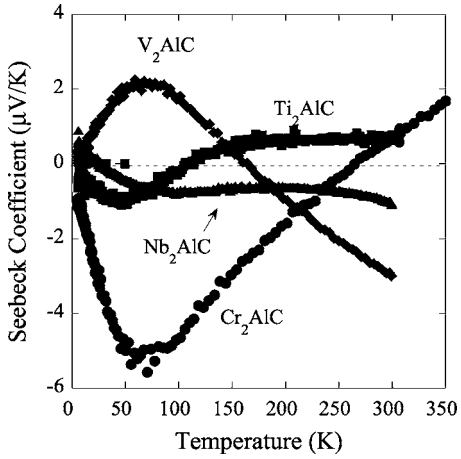

FIG. 4. Plot of Seebeck coefficients as a function of temperature.

In the two-band model the magnetoresistance $\Delta\rho/\rho = [\rho(H)-\rho(H=0)/\rho(H=0)]$ and the electrical conductivity σ are described by

$$\frac{\Delta\rho}{\rho} = \alpha B^2 = \frac{\mu_n\mu_p np(\mu_n+\mu_p)^2}{(n\mu_n + p\mu_p)^2}B^2, \tag{2}$$

$$\sigma = \frac{1}{\rho} = e(n\mu_n + p\mu_p). \tag{3}$$

To solve the problem an additional constraint is required. Given the small Seebeck and Hall coefficients it is reasonable to choose carrier concentrations that are temperature independent (a reasonable assumption for metals) and as important, based on previous work, roughly equal numbers for the densities of the electrons and holes.

Thus, solving the above expressions, assuming that $n=p$, we find that at all temperatures for the three materials with negative Hall coefficients, $\mu_p \sim 0.8-0.9\mu_n$. In Cr_2AlC, with its positive R_H, $\mu_p \sim 1.02\mu_n$. The temperature dependence of R_H is imbedded in the mobility. The required temperature-dependent mobilities are shown in Fig. 3(b).

The carrier concentrations for Ti_2AlC and Cr_2AlC are 1.0×10^{27} and 1.2×10^{27} m^{-3}, respectively; those for V_2AlC and Nb_2AlC are identical at 2.7×10^{27} m^{-3}. These values are quite reasonable and are comparable with those determined for the M_3AX_2 compounds, Ti_3SiC_2 and Ti_3GeC_2 ($\approx 2.0\times10^{27}$ m^{-3}) (Ref. 10) and Ti_3AlC_2 (≈ 1.5 to 2×10^{27} m^{-3}).[9] Not surprisingly, there is no correlation between n and p and $N(E_F)$.[12,18]

The results to date strongly suggest that the electronic properties of the *MAX* phases are dominated by the *d* orbitals of the *M* elements and that these properties are, in turn, comparable to those of the transition metals. With this in mind, it is thus useful to briefly summarize what is known about the transition metal electronic transport. According to Kulikov,[17] the resistivity of transition metals can be written in a fashion similar to the Bloch-Grüneisen by

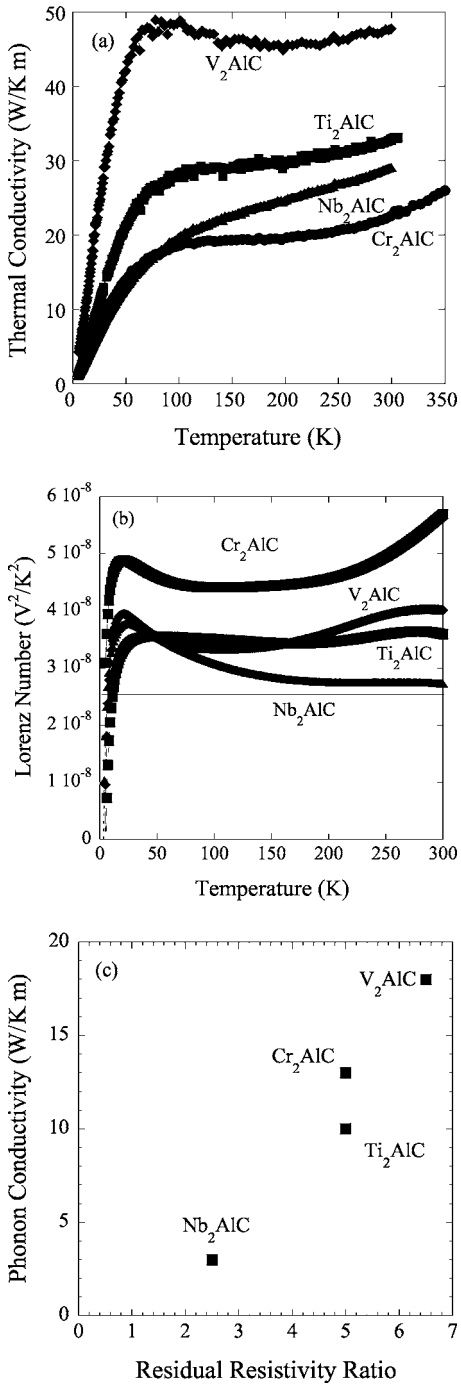

FIG. 5. (a) Temperature dependence of the thermal conductivity, κ. (b) Temperature dependence of Lorenz number. Note that the line near 2.5×10^{-8} V^2/K^2 is theoretical value for thermal conduction by charge carriers only. (c) Phonon conductivity, $\kappa_{ph}=(\kappa-L_0T/\rho)$ versus residual resistivity ratio, indicating that κ_{ph} is dominated by scattering.

$$\rho \propto \frac{1}{n\tau} \propto \frac{N(E_F)\lambda\Theta}{n}\left(\frac{T}{\Theta}\right)^5 J_5(\Theta/T), \tag{4}$$

where τ is the scattering time, $N(E_F)$ the density of states at the Fermi level, λ the electron-phonon coupling factor, $J_5(x)$ the Grüneisen integral, and Θ the Debye temperature. According to Eq. (4) and assuming Matthiessen's rule, $\mu(T=0)\propto\lambda(\mathrm{RRR}-1)/N(E_F)$ where $(\mathrm{RRR}-1)$ relates to the intrinsic resistivity. Plotting the electronic mobilities at 5 K as a function of $(\mathrm{RRR}-1)/N(E_F)$ [Fig. 3(c)] for the compounds tested in this work, together with previously reported corresponding values of other *MAX* phases[9,10] we find that there is a linear relationship, indicating that the electron-phonon coupling is more or less constant for all materials.

The sign of the Seebeck voltage is often used to qualitatively determine the sign of the dominant charge carrier. With this in mind, it may be expected that the Seebeck voltages should roughly reflect the sign and shape of R_H as a function of temperature. Comparing the Hall (Fig. 2) and the Seebeck (Fig. 4) coefficients it is clear there are no obvious correlations between them. Three of the materials have clearly changing signs of the Seebeck voltage with no corresponding changes in R_H, providing additional evidence that these compounds are nearly compensated.

B. Thermal properties

In agreement with a previous work, the *MAX* phases are good thermal conductors, because they are good electronic conductors. However, the results shown in Fig. 5(b), demonstrate that the total thermal conductivity has electronic and phonon contributions, κ_{el} and κ_{ph}, respectively. Since phonons are easily scattered by defects, especially in transition metal carbides and nitrides,[19] κ_{ph} should be sensitive to sample quality. One measure of defect density in a metal is the RRR. In Fig. 5(c), we plot $\kappa_{ph}=(\kappa-L_0T/\rho)$ calculated at room temperature as a function of RRR. It is clear that the differences in the thermal conductivities can be attributed to differences in the resistivities, which in turn are related to the density of states, and the defect density, which scatter both the phonons and charge carriers. To a lesser extent, the stiffness also plays a role, but only in compounds where κ_{ph} is large; viz. materials with high resistivities where κ_{el} is small or very clean materials, which provide a long phonon mean free path.

C. Elastic properties

Whereas the differences in the κ_{ph} values are more dependent on defect density than on the elastic properties, there are clear differences between the measured sound velocities in these compounds (Table I). They range from a high of $\approx$8500 m/s for Ti_2AlC to about 7000 m/s for Nb_2AlC. Most of these variations can be attributed to differences in density. The bulk moduli calculated in this work (column 8, Table I) are $\approx$25% lower than those recently directly measured in a diamond-anvil cell.[20]

Also included in Table I are recent *ab initio* calculations on the same compounds. With the notable exception of Cr_2AlC, the agreement between the calculated and measured elastic constants is quite good. This structural destabilization of Cr_2AlC was thus unexpected. It is in line, however, with other recent observations. As is noted above, it is seen in direct measurements of B.[20] It is also manifested in a 7% drop in the energy of the highest energy Raman vibrational

TABLE I. Young's E, shear G, and bulk B moduli of the M_2AlC phases. B and B^* are determined from velocity of sound and directly from diamond-anvil cell. Also listed are the longitudinal v_l and shear v_s sound velocities and Poisson ratio, ν. Θ_D^e corresponds to the Debye temperature calculated from the mean sound velocity, while Θ_D^T is that determined from low-temperature heat-capacity measurements.

Solid	Density g/cm^3	v_l (m/s)	v_s (m/s)	G (GPa)	E (GPa)	ν	B (GPa)	B^* (GPa)	Θ_D^e (K)	Θ_D^T (K)		$N(E_F)$ (1/eV unit cell)		References
Ti_2AlC	4.1	8525	5298	118	277	0.19	144	186[a]	732	672[b]	619[c]	4.9[b]	4.3[c]	This work
Theory	4.03	9133	5627	127	305	0.19	166		770					Ref. 24
V_2AlC	4.81	7989	4913	116	277	0.20	152	201[a]	696	625[b]	658[c]	7.5[b]	8.0[c]	This work
Theory	4.81	8863	5087	124	308	0.24	196		731					Ref. 24
Cr_2AlC	5.24	7215	4450	105	245	0.20	138	166[a]	644	589[b]	673[c]	14.5[b]	12.9[c]	This work
Theory	5.24	8939	5255	145	358	0.24	226		774					Ref. 24
Nb_2AlC	6.34	7125	4306	117	286	0.21	165	208[a]	577	NA	540[c]	NA	5.1[c]	This work
Theory	6.34	7573	4329	119	299	0.26	205		585					Ref. 24

[a]Reference 20.
[b]Reference 18.
[c]Reference 12.

mode—involving the motion of the A and M atoms along the c axis—of Cr_2AlC relative to the Ti-containing and V-containing structures[21]. Lastly, at $\approx 12\times10^{-6}$ K^{-1}, the thermal expansion coefficient of Cr_2AlC is $\approx$50% higher than that of either Ti_2AlC (Ref. 22) or Nb_2AlC.[23]

V. CONCLUSIONS

By measuring the electrical and thermal conductivities, Hall and Seebeck coefficients between 5 and 300 K of the Ti-, V-, Cr-, and Nb-containing M_2AlC phases, we have shown that, like other *MAX* phases, the electrical conductivities in these solids are compensated, with $n\approx p\approx 2\times10^{27}$ m^{-3}, and $\mu_n\approx\mu_p$ over the entire temperature range examined. Examining the mobility at 5 K, it was shown that the electron-phonon coupling of all studied *MAX* phases is more or less the same, irrespective of d element or structure. On the other hand, the phonon contribution to the total thermal conductivity was shown to be proportional to the defect concentration. We also measured the longitudinal and shear velocities of sound in these materials and have shown them to be elastically quite stiff.

ACKNOWLEDGMENTS

Partial support for this work from the National Science Foundation Grant No. DMR 0503711 is gratefully acknowledged. S.E.L. and J.D.H. acknowledge support from the New Jersey Commission on Higher Education and NSF Grant No. DMR 0114073.

*Current address: Thomson TWW Lancaster Research and Development Center, Lancaster, Pennsylvania 17601.

[1] M. W. Barsoum, Prog. Solid State Chem. **28**, 201 (2000).
[2] H. Nowotny, Prog. Solid State Chem. **2**, 27 (1970).
[3] P. Finkel, M. W. Barsoum, and T. El-Raghy, J. Appl. Phys. **87**, 1701 (2000).
[4] S. Myhra, J. W. B. Summers, and E. H. Kisi, Mater. Lett. **39**, 6 (1999).
[5] M. Sundberg, G. Malmqvist, A. Magnusson, and T. El-Raghy, Ceram. Int. **30**, 1899 (2004).
[6] M. W. Barsoum, L. H. Ho-Duc, M. Radovic, and T. El-Raghy, J. Electrochem. Soc. **150**, B166 (2003).
[7] H. I. Yoo, M. W. Barsoum, and T. El-Raghy, Nature (London) **407**, 581 (2000).
[8] M. W. Barsoum, H. I. Yoo, I. K. Polushina, V. Y. Rud, Y. V. Rud, and T. El-Raghy, Phys. Rev. B **62**, 10194 (2000).
[9] P. Finkel, M. W. Barsoum, J. D. Hettinger, S. E. Lofland, and H. I. Yoo, Phys. Rev. B **67**, 235108 (2003).
[10] P. Finkel, B. Seaman, K. Harrell, J. Palma, J. D. Hettinger, S. E. Lofland, A. Ganguly, M. W. Barsoum, Z. Sun, Sa Li, and R. Ahuja, Phys. Rev. B **70**, 085104 (2004).
[11] A. Ganguly, T. Zhen, and M. W. Barsoum, J. Alloys Compd. **36**, 287 (2004).
[12] S. E. Lofland, J. D. Hettinger, K. Harrell, P. Finkel, S. Gupta, M. W. Barsoum, and G. Hug, Appl. Phys. Lett. **84**, 508 (2004).
[13] S. Gupta and M. W. Barsoum, J. Electrochem. Soc. **151**, D24 (2004).
[14] I. Salama, T. El-Raghy, and M. W. Barsoum, J. Alloys Compd. **347**, 271 (2002).
[15] P. Finkel, J. D. Hettinger, S. E. Lofland, M. W. Barsoum, and T. El-Raghy, Phys. Rev. B **65**, 035113 (2001).
[16] J. C. Ho, H. H. Hamdeh, and M. W. Barsoum, J. Appl. Phys. **86**, 3609 (1999).
[17] N. I. Kulikov, J. Phys. F: Met. Phys. **8**, L137 (1978).
[18] M. K. Drulis, H. Drulis, S. Gupta, and M. W. Barsoum (unpublished).
[19] W. S. Williams, Prog. Solid State Chem. **6**, 57 (1971).
[20] B. Manoun, R. Gulve, S. K. Saxena, and M. W. Barsoum (unpublished).
[21] J. E. Spanier, S. Gupta, M. Amer, M. W. Barsoum, Phys. Rev. B

71, 012103 (2005).
[22] M. W. Barsoum, M. Ali, and T. El-Raghy, Metall. Mater. Trans. A **31A**, 1857 (2000).
[23] M. W. Barsoum, I. Salama, T. El-Raghy, J. Golczewski, W. D. Porter, H. Wang, H. J. Seifert, and F. Aldinger, Metall. Mater. Trans. A **33A**, 2779 (2002).
[24] Z. Sun, S. Li, R. Ahuja, and J. M. Schneider, Solid State Commun. **129**, 589 (2004).